Tunneling quantum correction potential model for drift-diffusion simulations of Schottky contact resistance

A. -T. Pham [a], M. A. Pourghaderi [b], S. Jin [a], S. Song [b], Y. Park [b], U. Kwon [b], W. Choi [a], D. S. Kim [b]
[a] TCAD lab, Samsung Semiconductor Inc., San Jose, CA, USA.
[b] CSE team, Innovation center, Samsung Electronics, Korea.

2024 International Conference on Simulation of Semiconductor Processes and Devices (SISPAD) | 979-8-3315-1635-2/24/$31.00 ©2024 IEEE | DOI: 10.1109/SISPAD62626.2024.10733338

***Abstract*— A new approach based on tunneling quantum correction potential is proposed for Schottky contact resistance simulation. The new model relies on a quantum correction potential retaining the conduction band edge near the Schottky interface while avoiding non-local mesh and Wentzel-Kramers-Brillouin computation for direct tunneling treatment. The new model is implemented into the drift-diffusion solver. The accuracy of new model is much higher than the accuracy of Schottky distributed resistance vs non-local tunneling model for a wide range of Si doping concentrations. For typical IV characteristic simulations, the new method is faster than the non-local tunneling model method by up to 4 times.**

I. Introduction

The performance of advanced logic cells is largely determined by parasitic components. Despite the complex process and design solutions to minimize their impact, some of the parasitic components remain fixed by intrinsic material properties. A prime example of this category is Schottky contact resistance which naturally occurs at any metal-semiconductor interface. For example, in the case of titanium silicide, the n-type Schottky barrier height (SBH) is broadly reported to be around 0.5 eV, decided by the chemistry of silicon, titanium silicide, and their interface. In practice, electrons from the highly doped silicon region must tunnel through such a high SBH to reach to the bulk of metal contact. To model Schottky contact within the drift-diffusion (DD) framework, very often, the non-local tunneling (NLT) method based on the Wentzel-Kramers-Brillouin (WKB) integration approach is used [1]. The NLT method involves (i) the non-local mesh establishment aligned with a predefined tunneling path, (ii) the WKB approximation for the calculation of tunneling probability along the tunneling path. Such an approach involves many computational steps, resulting in a long turnaround time (TAT). On top of that, the non-local treatment can degrade the coupling of the system matrix, leading to slow convergence and numerical instability of the DD solver.

An alternative method has been proposed based on Schottky distributed resistance (SDR) [2]. However, the SDR method flattens the conduction band edge (CBE), altering the electrostatics near the Schottky contact. This simplification inhibits the formation of depletion regions and correct potential profile in scaled devices.

In this work, a new approach based on tunneling quantum correction potential (TVqc) is proposed, through which the precise CBE profile near Schottky contact is retained. Relying on a quantum correction potential, the TVqc method is fully local. Therefore, nonlocal mesh and WKB computation are avoided. In this way, the TVqc model offers much better numeric efficiency than NLT, while preserving the same level of accuracy.

In the next section, the tunneling quantum correction potential model is described. The calibration and simulation results for 1D and 2D devices are shown thereafter. And finally, the conclusion is drawn.

II. Tunneling quantum correction potential model

Due to the natural band offset and resulting barrier across the contact, the certain extent of semiconductor region near the interface gets depleted from the carriers. In conventional DD framework, such a carrier profile results in substantial resistance. To correct this DD artifact, the current should be boosted with controlled adjustment of local density. In this light, the TVqc model employs a quantum correction potential which boosts carrier density at the Schottky contact. Using TVqc model, the profile of potential barrier is kept precise while tunneling quantum correction pumps controlled amount of carrier toward the Schottky interface and mimics the tunneling current. The tunneling quantum correction potential is given by:

$$\Lambda_{\mathrm{tunneling}}(\vec{r}) = -\Phi_{\mathrm{B,tunneling}} \cdot \exp\left(-\frac{|\vec{r}-\vec{r}_0|}{L(N(\vec{r}))}\right) \quad (1)$$

where $\Phi_{\mathrm{B,tunneling}}$ is effective tunneling SBH. For a local position vector $\vec{r}$ in the device domain, $\vec{r}_0$ is a position vector on the Schottky interface, which is nearest to $\vec{r}$. $L(N)$ is doping dependent decay length, given by:

$$L(N) = \frac{L_0}{1+\exp[\alpha(x-x_1)]} + \frac{L_\infty}{1+\exp[-\alpha(x-x_1)]} \quad (2)$$

$$x = \log_{10}\frac{N}{N_0}, \quad x_1 = \log_{10}\frac{N_1}{N_0}, \quad N_0 = 1\mathrm{cm}^{-3} \quad (3)$$

Here, L_0 and L_∞ are decay lengths at vanishing and infinite doping, respectively. N is absolute doping level at position $\vec{r}$. N_1 is transitional doping concentration. $\Phi_{\mathrm{B,tunneling}}$, N_1, and α are model parameters. To consider the orientation dependence of contact resistivity, orientation dependence of $\Phi_{\mathrm{B,tunneling}}$ and α is enabled.

To enable the TVqc model, $\Lambda_{\mathrm{tunneling}}(\vec{r})$ given by (1) is directly added to the conventional quantum correction term of

the density gradient model [3]. In this way, the self-consistent solution of Poisson, continuity, and density gradient equations produces the desired tunneling component.

III. Results

For calibration, the model parameters of TVqc, NLT, and SDR models are adjusted to match the contact resistance of 1D metal/Si structure vs DFT-NEGF reference data. The DFT reference data is prepared for (100) and (111) silicon orientation in contact with amorphous titanium silicide, where n-SBH of samples reads as 0.5 and 0.57eV, respectively. Fig. 1 shows that TVqc, NLT, and SDR models match well the DFT-NEGF results for contact resistance vs n-type doping concentration ranging from 3e19 to 3e21 cm^{-3} for (100) and (111) metal/Si interfaces.

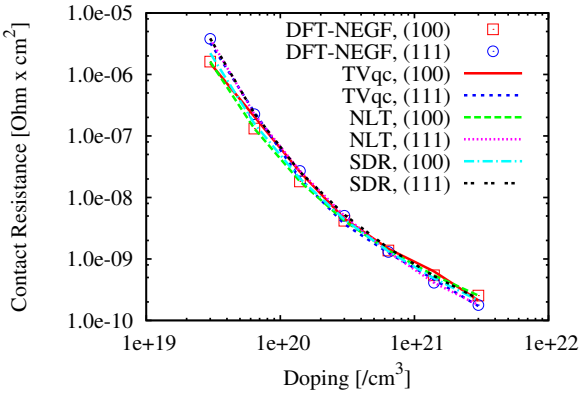

Fig. 1. Contact resistance vs n-type doping concentration calculated by TVqc, NLT, and SDR models vs DFT-NEGF method for (100) and (111) metal/Si interfaces.

Fig. 2 (top) depicts the TVqc model results for CBE, tunneling quantum correction potential ($\Lambda_{\text{tunneling}}(x)$), and quantum potential in a Schottky contact with N_D = 1.4e20 cm^{-3} and (100) metal/Si interface. The CBE resulting from TVqc model agrees well with the NLT model result.

Note that, in the TVqc model, the $\Lambda_{\text{tunneling}}(x)$ is in opposite sign vs CBE (Fig. 2 (top)), in order to boost the carrier density near the Schottky interface (Fig. 2 (top)). Excluding $\Lambda_{\text{tunneling}}(x)$ from the carrier density calculation, electron density from the TVqc model (shown as eDensity0 in Fig. 2 (bottom)) are in good agreement with the NLT model result.

2D dog-bone nFETs (Tch=5nm, Lch=15nm, Tsd=15nm, Lsd=15nm, Nch=1e15 cm^{-3}, Nsd=5e20 cm^{-3}, Nct=5e19-5e20 cm^{-3}, (001) surface/<110> channel) with Schottky S&D contacts (Fig. 3) is simulated using DD approach with NLT, TVqc, and SDR models, which are well calibrated from the previous step. S&D doping concentration (Nsd) is kept as high as 5e20 cm^{-3} in order to reduce the access resistance. Within a 1nm thicknes layer around S&D contacts, the doping

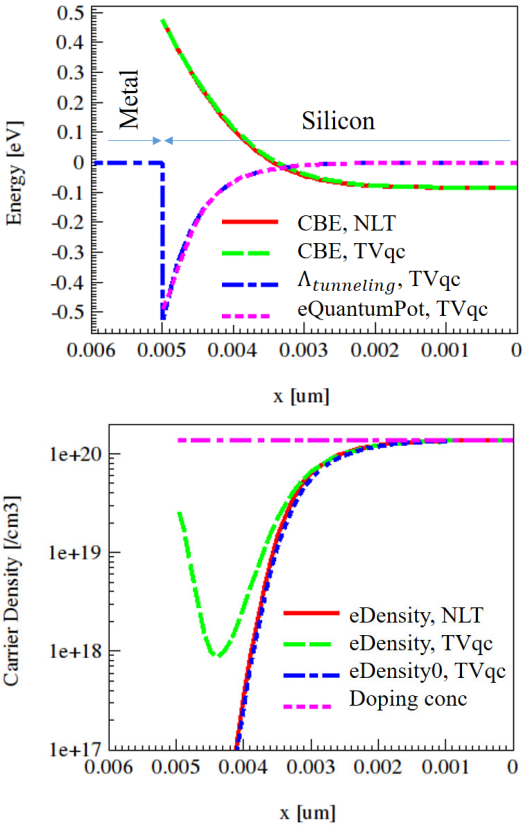

Fig. 2. Conduction band edge (CBE), tunneling quantum correction potential ($\Lambda_{\text{tunneling}}(x)$), quantum potential (top), electron density (eDensity) and doping profile (bottom) in a Schottky contact with N_D = 1.4e20 cm^{-3} and (100) metal/Si interface.

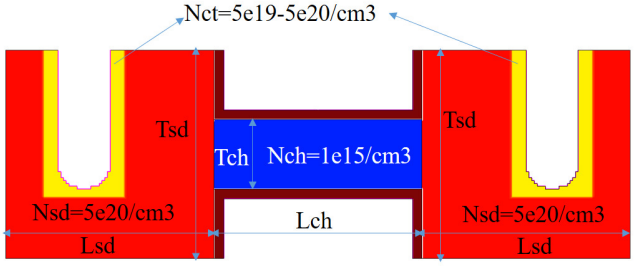

Fig. 3. Doping profile of 2D dog-bone nFETs.

concentration is overidden with Nct=5e19-5e20 cm^{-3}, for investigating the contact resistance effects.

For TVqc model, Fig. 4 shows tunneling quantum correction potential (top) and quantum potential (bottom) profiles for Nct=5e19 cm^{-3} with V_{DS} = 50mV, V_{GS} = 0.8V. Tunneling quantum correction potential exponently decays from the S&D contacts and vanishes inside the channel. Therefore, this pattern is reflected in total quantum potential around the contact region. Inside the channel, however, total quantum potential retains high value in order to take care of electron quantum confinement effects.

For V_{DS} = 0.7V, V_{GS} = 0.8V, the doping profile (a1-3), CBE (b1-3), and electron quasi-Fermi energy (c1-3) resulting

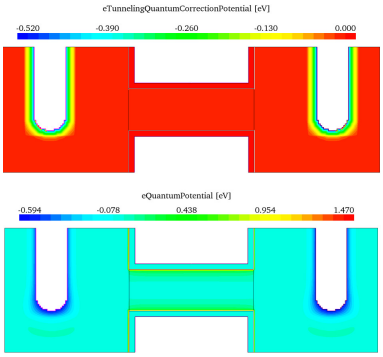

Fig. 4. Tunneling quantum correction potential (top) and quantum potential (bottom) profiles in TVqc model for Nct=5e19 cm^{-3}. $V_{\rm DS}$ = 50mV, $V_{\rm GS}$ = 0.8V.

from NLT, TVqc, and SDR models are shown in Fig. 6 and 5 for Nct=5e19 and Nct=3e20 cm^{-3}, respectively. While NLT and TVqc models give similar CBE as well as electron quasi-Fermi energy, the results from the SDR model near Schottky contact are remarkably different for Nct as low as 5e19 cm^{-3}. Particularly in scaled devices, such details are crucial for accurate electrostatic and device performance analysis.

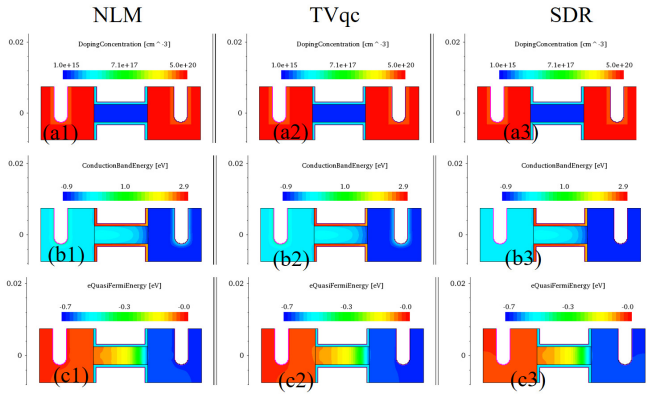

Fig. 5. Doping profile (a1, a2, a3), conduction band edge (b1, b2, b3), electron quasi-Fermi energy (c1, c2, c3) resulting from NLT (a1, b1, c1), TVqc (a2, b2, c2), and SDR (a3, b3, c3) models. $V_{\rm DS}$ = 0.7V, $V_{\rm GS}$ = 0.8V. Nct=3e20 cm^{-3}.

Next, the impact of model on $I-V$ characteristics is explored. For a high level of Nct=3e20 cm^{-3}, $I_{\rm D}-V_{\rm GS}$ characteristics (shown in Fig. 7) resulting from NLT, TVqc, and SDR models are in excellent agreement for both $V_{\rm DS}$ = 50mV and $V_{\rm DS}$ = 0.7V biases.

When Nct reduces to 5e19 cm^{-3}, TVqc model still gives good match of $I_{\rm D}-V_{\rm GS}$ characteristics (shown in Fig. 8) resulting from NLT model for both $V_{\rm DS}$ = 50mV and $V_{\rm DS}$ = 0.7V biases. However, SDR fails to produce reference results in low and high bias condition. With ideal Ohmic contact, $I_{\rm D}$ is up to 42% higher than the $I_{\rm D}$ with Schottky contact, emphasizing the importance of parasitic contact resistance.

In summary, as depicted in Fig. 9, $I_{\rm D}-V_{\rm DS}$ characteristics resulting from NLT, TVqc, SDR models for $V_{\rm GS}$ = 0.8V are in excellent agreement for Nct=3e20 cm^{-3} (top). For Nct=5e19 cm^{-3} (bottom), the error of TVqc vs NLT model is small ($<10\%$) while the error of SDR vs NLT model is much bigger, up to 500%.

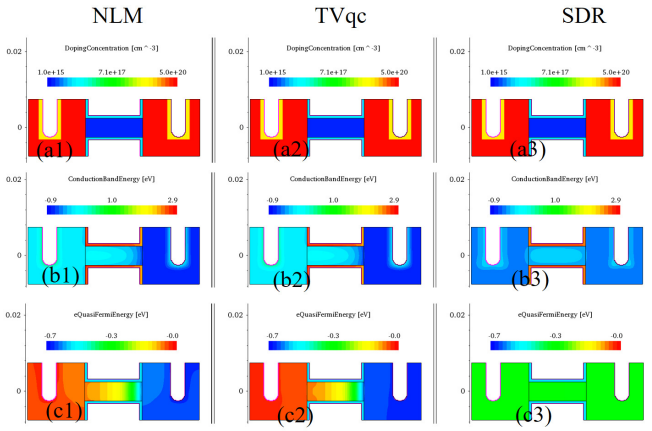

Fig. 6. Doping profile (a1, a2, a3), conduction band edge (b1, b2, b3), electron quasi-Fermi energy (c1, c2, c3) resulting from NLT (a1, b1, c1), TVqc (a2, b2, c2), and SDR (a3, b3, c3) models. $V_{\rm DS}$ = 0.7V, $V_{\rm GS}$ = 0.8V. Nct=5e19 cm^{-3}.

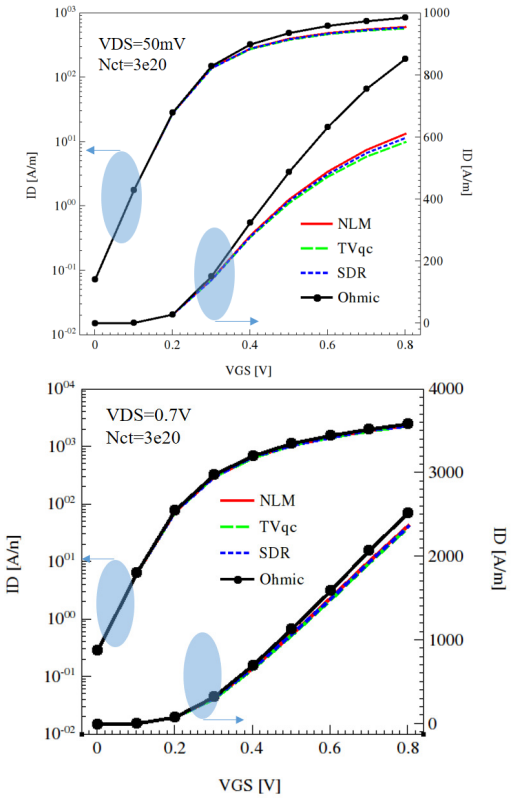

Fig. 7. $I_{\rm D}-V_{\rm GS}$ characteristics with Schottky contact NLT, TVqc, SDR models vs $I_{\rm D}-V_{\rm GS}$ characteristics with ideal Ohmic contact for $V_{\rm DS}$ = 50mV (top) and $V_{\rm DS}$ = 0.7V (bottom). Nct=3e20 cm^{-3}.

Fig. 10 shows $I_{\rm D}$ vs Nct characteristics for $V_{\rm GS}$ = 0.8V with Schottky contact NLT, TVqc, SDR models vs $I_{\rm D}$ with ideal Ohmic contact for $V_{\rm DS}$ = 50mV and $V_{\rm DS}$ = 0.7V. For a wide range of Nct, TVqc model results are good agreement with NLT model. However, SDR model can only retain decent

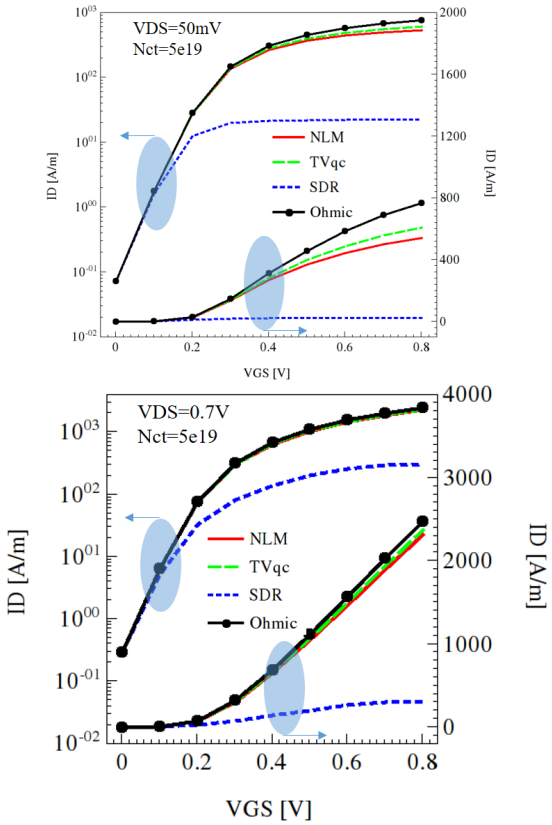

Fig. 8. $I_{\mathrm{D}} - V_{\mathrm{GS}}$ characteristics with Schottky contact NLT, TVqc, SDR models vs $I_{\mathrm{D}} - V_{\mathrm{GS}}$ characteristics with ideal Ohmic contact for $V_{\mathrm{DS}} = 50\mathrm{mV}$ (top) and $V_{\mathrm{DS}} = 0.7\mathrm{V}$ (bottom). Nct=5e19 cm^{-3}.

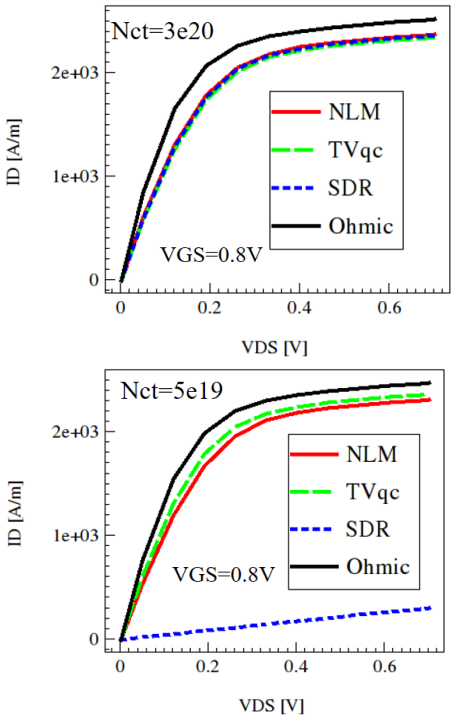

Fig. 9. $I_{\mathrm{D}} - V_{\mathrm{DS}}$ characteristics with Schottky contact NLT, TVqc, SDR models vs $I_{\mathrm{D}} - V_{\mathrm{DS}}$ characteristics with ideal Ohmic contact for Nct=3e20 cm^{-3} (top) and Nct=5e19 cm^{-3} (bottom). $V_{\mathrm{GS}} = 0.8\mathrm{V}$.

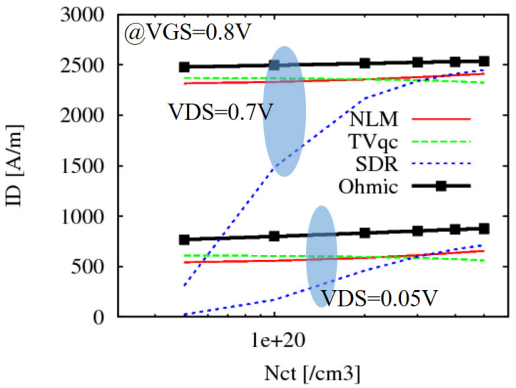

Fig. 10. I_{D} vs Nct characteristics with Schottky contact NLT, TVqc, SDR models vs I_{D} with ideal Ohmic contact for $V_{\mathrm{DS}} = 50\mathrm{mV}$ and $V_{\mathrm{DS}} = 0.7\mathrm{V}$. $V_{\mathrm{GS}} = 0.8\mathrm{V}$.

match against NLT results for Nct higher than 1e20 cm^{-3}. Below this limit, the error significantly increases.

Turn around time (TAT)-wise, TVqc matches the performance of SDR model. Compared to NLT, TVqc is faster by about three (for $V_{\mathrm{DS}} = 0.7\mathrm{V}$) to four times (for $V_{\mathrm{DS}} = 50\mathrm{mV}$) thanks to the fast convergence and numerical stability of the TVqc model implemented in the DD solver.

IV. Conclusion

A new approach based on tunneling quantum correction potential is proposed for Schottky contact resistance simulation. The TVqc model relies on a quantum correction potential retaining the CBE near the Schottky interface while avoiding non-local mesh and WKB computation for direct tunneling treatment. The TVqc model can be implemented into the DD solver in a straightforward manner. The error of TVqc is shown to be much smaller than the error of SDR vs NLT model for a wide range of Si doping concentrations, specifically $<$1e20 cm^{-3}. For typical IV characteristic simulations, the TVqc method is faster than the NLT method by 3$\sim$4 times.

References

[1] Y. Ando and T. Itoh, "Calculation of transmission tunneling current across arbitrary potential barriers," *J. Appl. Phys.*, vol. 61, pp. 1497–1502, 1987.

[2] K. Varahramyan and E. Verret, "A model for specific contact resistance applicable for titanium silicide-silicon contacts," *Solid-State Electronics*, vol. 39, no. 11, pp. 1601–1607, 1996.

[3] E. Lyumkis, R. Mickevicius, O. Penzin, B. Polsky, K. E. Sayed, A. Wettstein, and W. Fichtner, "Simulation of ultrathin, ultrashort double-gated MOSFETs with the density gradient transport model," in *Intl. Conference on Simulation of Semiconductor Processes and Devices*, Kobe, Sep. 2002, p. 271.